Spatio-temporal modelling of the first Chikungunya epidemic in an intra-urban setting: the role of socioeconomic status, environment and temperature

Laís Picinini Freitas[1,2*], Alexandra M. Schmidt[3], William Cossich[4], Oswaldo Gonçalves Cruz[2], Marilia Sá Carvalho[2]

[1] Programa de Pós-Graduação em Epidemiologia em Saúde Pública, Escola Nacional de Saúde Pública Sergio Arouca (ENSP), Oswaldo Cruz Foundation, Rio de Janeiro, Brazil

[2] Programa de Computação Científica (PROCC), Oswaldo Cruz Foundation, Rio de Janeiro, Brazil

[3] Department of Epidemiology, Biostatistics and Occupational Health, McGill University, Montreal, Canada

[4] Department of Physics and Astronomy, University of Bologna, Bologna, Italy

* Corresponding author

E-mail: lais.picinini.freitas@gmail.com (LPF)

Abstract

Three key elements are the drivers of *Aedes*-borne disease: mosquito infestation, virus circulating, and susceptible human population. However, information on these aspects are not easily available in low- and middle-income countries. We analysed data on factors that influence one or more of those elements to study the first chikungunya epidemic in Rio de Janeiro city in 2016. Using spatio-temporal models, under the Bayesian framework, we estimated the association of those factors with chikungunya notified cases by neighbourhood and week. To estimate the minimum temperature effect in a non-linear fashion, we used a transfer function considering an instantaneous effect and propagation of a proportion of such effect to future times. The sociodevelopment index and the proportion of green areas were included in the model with time-varying coefficients, allowing us to explore how their associations change throughout the epidemic. There were 13627 chikungunya cases in the study period. The sociodevelopment index presented the strongest association, inversely related with the risk of cases. Such association was more pronounced in the first weeks, indicating that socioeconomically vulnerable neighbourhoods were affected first and hardest by the epidemic. The proportion of green areas effect was null for most weeks. The temperature was directly associated with the risk of chikungunya for most neighbourhoods, with different decaying patterns. The temperature effect persisted longer where the epidemic was concentrated. In such locations, interventions should be designed to be continuous and to work in the long term. We observed that the role of the covariates change over time. Therefore, time-varying coefficients should be widely incorporated when modelling *Aedes*-borne diseases. Our model contributed to the understanding of the spatio-temporal dynamics of an urban *Aedes*-borne disease introduction in a tropical metropolitan city.

Author Summary

Viruses transmitted by the *Aedes* mosquitoes represent a major public health concern. With the abundance of the mosquito and susceptible human population, the entry of new *Aedes*-transmitted virus brings the risk of large epidemics. The first-ever chikungunya epidemic in Rio de Janeiro city, Brazil, happened in 2016. We used information neighbourhood information on environment, socioeconomic status, and weekly temperature, to study the disease spread within the city. Our results show that better socioeconomic status play a major role in preventing the disease, with poorer areas being affected first and harder by the epidemic. This highlights that improving socioeconomic and sanitary conditions are essential for *Aedes*-borne diseases prevention and control. The temperature increased the risk of chikungunya cases, and this effect persisted for longer in areas where the epidemic was concentrated. This indicates that interventions should be designed to be long-lasting in such locations. Our results contribute to understanding better the dynamics of a first urban *Aedes*-borne disease epidemic in a tropical metropolitan city, with the potential to help design better interventions for disease prevention and control.

Introduction

The first chikungunya virus (CHIKV) epidemic in Rio de Janeiro city, the second most populated city in Brazil and its leading tourist destination, occurred in 2016 [1]. CHIKV is transmitted to humans by the same vectors as dengue viruses (DENV), the *Aedes* mosquitoes [2]. Vector-control activities have not prevented Rio de Janeiro from being endemic for dengue for years, nor from having experienced large dengue epidemics every three to four years, in general [3–5].

For a chikungunya epidemic to occur, three main elements are necessary, represented by the blue area in Fig 1: mosquito population, susceptible human population, and the virus circulating [6–8]. The *Ae. aegypti* mosquito is present all over the city of Rio de Janeiro, facilitating a new arbovirus is established. Because CHIKV and DENV belong to different families, previous immunity to DENV does not cross-react with CHIKV, and the population of Rio de Janeiro can be considered equally naïve to CHIKV before 2016. Therefore, given the presence of the mosquito population and susceptible human population, the occurrence of local CHIKV transmission in Rio de Janeiro was conditioned by the entry of the virus. Once the virus is circulating and established, how it will spread within the city depends on multiple factors. As a consequence, some areas of the city will experience the epidemic at different times, and will also have different attack rates.

Fig 1. A theoretical model for a chikungunya epidemic in a given region. Direct associations are represented by black arrows and indirect associations by red arrows. The blue area includes the necessary elements for the epidemic to occur.

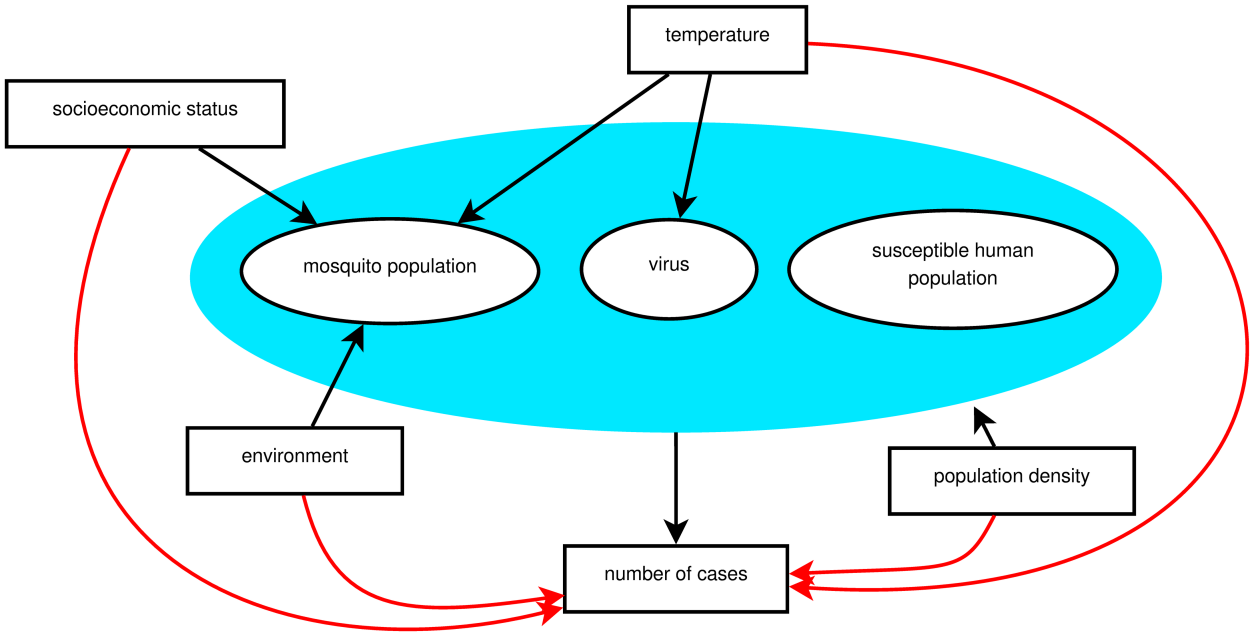

Reliable data regard to the intra-urban level of vector population, the susceptible human population over time, and the entry time of the virus in each location are necessary to understand the spatio-temporal dynamics of an epidemic. However, these data are not usually available. Alternatively, measured factors – such as temperature, socioeconomic and environmental factors – indirectly associated with the number of chikungunya cases (represented by red arrows in Fig 1) can be used as proxies. These factors have a direct effect (represented by black arrows in Fig 1) on the necessary elements for an epidemic to occur (inside the blue area), which are unmeasured. The temperature varies with time, and also present different effects on the epidemic over time. Socioeconomic and environmental characteristics take long periods to show important changes and can be considered fixed during the period of an epidemic. However, the way these factors impact the number of cases can change as the epidemic progresses, i.e., with time-varying effects.

The temperature affects the *Ae. aegypti* population, the virus, and the mosquito-virus interaction [9]. Ideal temperature conditions accelerate all stages of the mosquito life cycle, increasing the population in the long term. In the short term, the temperature influences the mosquito activity as well as the length of the virus incubation period, with maximal transmission occurring around 26–29°C [10]. Regarding the environment, the *Ae. aegypti* mosquitoes are highly adapted to urban settings, and the level of urbanisation is inversely correlated with the proportion of green areas [11]. The socioeconomic status impacts the mosquito population as disorderly urbanisation and inadequate sanitary conditions favour the presence of the mosquito most common reproduction site: containers filled with water found inside or in the surroundings of domiciles [12,13]. Furthermore, high population densities favour the contact between the mosquito and the human, increasing the chance of infection and transmission [14].

In the last decades, models that take into account the spatial dependency structure of the cases have been applied to better estimate covariates' association with *Aedes*-borne diseases epidemics [15–18]. The application of spatial models for intra-urban settings is growing more recently [19–22]. These model types, as the intrinsic conditional autoregressive (ICAR) models [23], are built under the assumption that adjacent areas share similar characteristics. The inclusion of a latent spatial random effect accounts for both the spatial structure and unmeasurable factors [24]. The inclusion of time-varying coefficients allows us to explore how the effect of the covariates change throughout the epidemic. The temperature is usually included in statistical models for *Aedes*-borne diseases in a linear fashion and with a pre-defined lag. We propose to estimate the temperature effect in a non-linear framework using a transfer function, including an immediate effect and a memory effect that propagates to future times. Another advantage of using a transfer function is that the estimation of the lag of the effect is data-driven [25].

We used this methodological approach (ICAR models with time-varying coefficients and a transfer function) to identify how temperature, socioeconomic and environmental factors are related

to the space-time progression of an *Aedes*-borne disease epidemic in an intra-urban setting. The first chikungunya epidemic in Rio de Janeiro, a large tropical city with environmental and socioeconomic disparities, presents ideal conditions to this end.

Methods

Study site

Rio de Janeiro is the second-largest city in Brazil, with 6,3 million inhabitants (2010), and its primary tourist destination. Rio's area is of 1204 km², with 160 neighbourhoods grouped into four large regions (Downtown, South, North and West). These regions are subdivided in 10 health districts called programmatic areas: area 1.0 (Downtown region); areas 2.1 and 2.2 (South region); areas 3.1, 3.2, 3.3 (North region); and areas 4.0, 5.1, 5.2 and 5.3 (West region) (Fig 2).

Fig 2. Rio de Janeiro city by programmatic areas and neighbourhoods, 2010, Brazil.

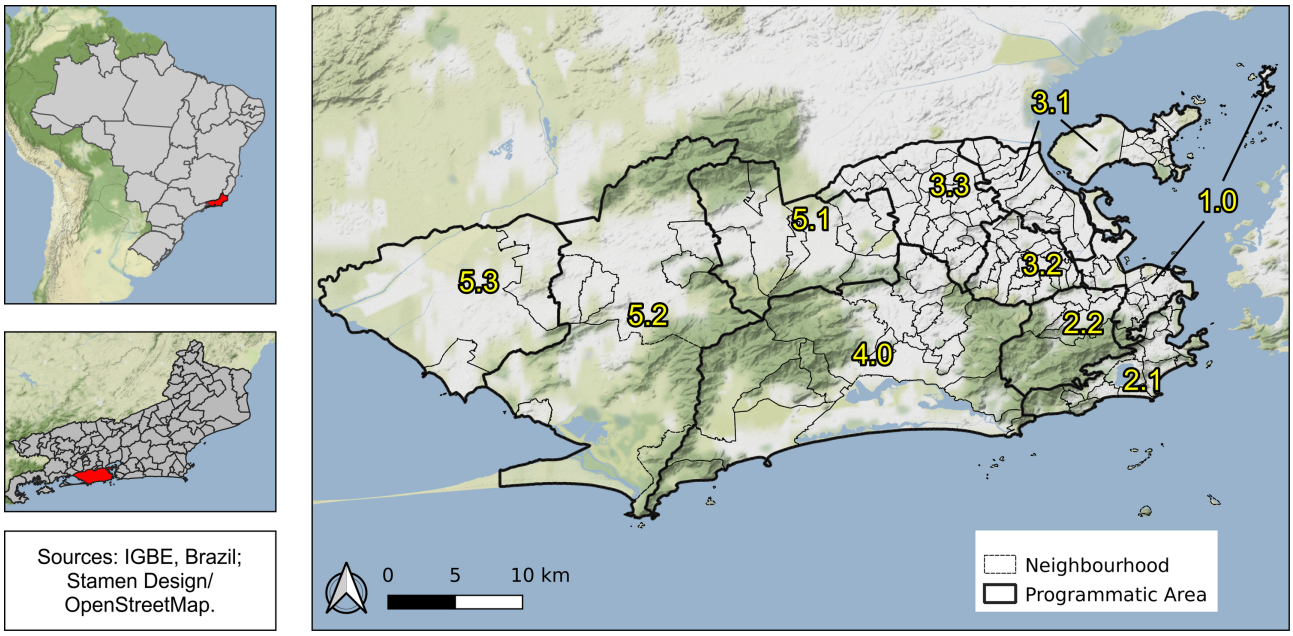

With three mountain massifs and 84 km of beaches, Rio has a diverse geography that is directly associated with the history of occupation and with socioeconomic disparities [26]. The Downtown region is the historical, commercial and financial centre of the city, with many cultural

127 establishments. The South region is the most popular tourist destination, with famous beaches and
128 wealthy neighbourhoods. In the North region, there are very large slums ("*favelas*") and nearly 27%
129 of the population, almost 2.4 million people, live in such communities [27]. The West region has
130 more heterogeneous characteristics among its neighbourhoods, being the area 5.1 more densely
131 populated, areas 5.2 and 5.3 less urbanised, and area 4.0 wealthier.
132
133 **Data**
134 *Chikungunya cases*
135 Data on chikungunya cases were obtained from the Notifiable Diseases Information System
136 (SINAN) via the Rio de Janeiro Municipal Secretariat of Heath and are publicly available [28].
137 We analysed notified cases of chikungunya (confirmed by laboratory or clinical-
138 epidemiological criteria) occurring in Rio de Janeiro municipality between January and December
139 2016, by week and neighbourhood of the patient's residence.
140 Case definitions follow the Ministry of Health protocols. A suspected case of chikungunya is
141 defined as a patient with sudden fever of over 38.5°C and severe arthralgia or arthritis not explained
142 by other conditions, and who either lives in endemic areas or has visited one up to two weeks before
143 the onset of symptoms or has an epidemiological link with a confirmed case. A confirmed case is a
144 suspected case with at least one positive specific laboratory test for CHIKV or confirmed by
145 clinical-epidemiological criteria [29].
146 *Socioeconomic data*
147 To characterise the socioeconomic status, we obtained the sociodevelopment index data by
148 neighbourhood from the *Instituto Pereira Passos* [30]. This index is based on eight indicators from
149 the 2010 Demographic Census: 1) the percentage of domiciles with adequate water supply; 2) the
150 percentage of domiciles with adequate sewage; 3) the percentage of domiciles with garbage
151 collection; 4) the average number of toilets per resident; 5) the percentage of illiteracy among

residents between 10 and 14 years old; 6) per capita income of the domiciles, expressed as minimum wages; 7) the percentage of domiciles with per capita income up to one minimum wage, and 8) the percentage of domiciles with per capita income greater than five minimum wage. The sociodevelopment index is calculated as the arithmetic average of the normalised indicators (each ranging from 0 to 1, being 0 the worst socioeconomic condition and 1, the best) [30].

We also obtained data on the population by neighbourhood from the *Instituto Pereira Passos* [31].

Environment and temperature data

Land use data for the city of Rio de Janeiro were obtained from the *Instituto Pereira Passos* as a shapefile [32]. We created the category “green areas” by aggregating: agricultural areas, areas with swamps and shoals, areas with tree and shrub cover, and areas with woody-grass cover. After that, we calculated the proportion of green areas for each neighbourhood (Fig 4B).

Temperature information for 2016 was obtained from 38 meteorological weather stations in Rio de Janeiro, from five different meteorological and environmental institutes. The institutes are the Brazilian National Institute of Meteorology [33], the Brazilian Airspace Control Department [34], the Rio de Janeiro State Environmental Institute [35], the Rio de Janeiro Municipal Environmental Secretariat [36] and the *Alerta Rio* System [37]. All measurements are made according to the recommendations of the World Meteorological Organization [38]. The institutes make their meteorological data publicly available, being that the frequency of measurements of the first four organisations is hourly, while the *Alerta Rio* System measurements are made every 15 minutes.

From the temperature measurements, we computed the daily maximum, minimum and mean temperature. We also evaluated the availability of daily data in terms of missing measurements. The daily records that had more than 60% of missing measurements were excluded. We decided to use the minimum temperature as in tropical climates it acts as a limiting factor for the *Ae. aegypti*

activity and population [39,40]. We then obtained the minimum temperature for each week and station, and, to obtain the minimum temperature by neighbourhood, we applied universal kriging. Briefly, kriging is a method that uses a sample of data points to estimate the value of a given variable over a continuous space [41]. First, we interpolated the minimum temperature to a grid with each unit measuring 500m x 500m. The grid with the meteorological weather stations locations is displayed in the S1 Fig. Then we obtained the minimum temperature of the neighbourhood by calculating the average of the minimum temperature of the grid units whose centroids were within the boundaries of the neighbourhood.

To process and organise the environmental data, we used R version 3.6.1 [42] and packages sf [43], geoR [44] and tidyverse [45].

Statistical analysis

We used the Stan platform [46,47] to fit spatio-temporal models, more specifically ICAR models, to a dataset consisting of neighbourhoods counts of chikungunya cases, exploring the relationship with sociodevelopment index, the proportion of green areas and minimum temperature. Let $Y_{i,t}$ be the counts of chikungunya cases at neighbourhood i = 1, 2, …, n = 160, and week t = 1, 2, … , T, where $Y_{i,t} \sim Poisson(\mu_{i,t})$. We explored different structures for $\mu_{i,t}$, presented in the S1 Appendix along with each Watanabe-Akaike information criterion (WAIC) [48]. The model selected based on the WAIC has the following structure:

$$\log(\mu_{i,t}) = \log(e_i) + \beta_0 + X'_i\beta_{k,t} + U_{i,t} + \phi_i$$
$$U_{i,t} = \rho_i U_{i,t-1} + \zeta_i Temperature_{i,t} \qquad (1)$$

The latent spatial effect is represented by ϕ, which, a *priori*, follows a conditional autoregressive distribution [23]; that is, the conditional distribution of each ϕ_i follows a normal distribution whose mean and variance depend on the neighbourhood structure w_{ij}. Assuming a binary neighbourhood structure, where w_{ij}=1 if areas i and j share borders and 0 otherwise, each ϕ_i

follows a conditional normal distribution whose mean is equal to the average of its neighbours, and its variance is inversely proportional to the number of neighbours d_i, that is:

$$p(\phi_i|\phi_{i\sim j}) = N\left(\frac{\sum_{i\sim j}\phi_i}{d_i}, \frac{\sigma^2}{d_i}\right) \quad (2)$$

The expected number of chikungunya cases at neighbourhood i (e_i) represents the number of cases that would have been observed if there were no differences in the incidence of cases across time and space:

$$e_i = \left(\frac{\sum_{i=1}^{n}\sum_{t=1}^{T} Y_{i,t}}{\sum_{i=1}^{n} population_i} population_i\right)/T \quad (3),$$

β_0 is the intercept, X'_i represents a vector of k covariates and $\beta_{k,t}$ *is* the coefficient of covariate k in week t. We decided to allow for time-varying coefficients for the covariates to explore if their association with the number of cases vary as the epidemic progresses. The covariates included in the X'_i vector were sociodevelopment index and proportion of green areas. The proportion of green areas showed a skewed distribution. Therefore, this variable was transformed to the cubic root. We also fitted models including the population density. However, the 90% credible interval (CI) of the population density coefficient included 0 for most weeks, and the inclusion of this variable increased the WAIC . Therefore, the population density was not considered in the final model.

We estimated the temperature effect in a non-linear fashion using a transfer function ($U_{i,t}$), considering that the temperature has an immediate effect (ζ_i) and that a proportion (ρ_i) of this effect propagates to future times. This proportion ρ_i is called memory effect and we considered it to be any value between 0 and 1 [25]. To combine and visualise both effects of the temperature, we obtained the impulse response function of the temperature for each neighbourhood. This function expresses the effect of a 1 unit increase in the temperature of one week propagating in time [25]. The temperature was standardised.

The models were fitted under the Bayesian framework using the Stan platform [46,47] to run four chains of 10000 iterations each where the first 5000 were the warmup. Relatively vague, proper prior distributions were used. We visually inspected the chains and used the R-hat statistic to check convergence [46,49]. Model validation was performed by comparing the fitted number of cases (mean and 90% CI) with the observed number of cases [48]. It is worth mentioning that we also fitted models that considered the reparametrisation of the Besag-York-Mollié (BYM2) as proposed by Riebler et al. [50]. However, the random component was over 90% spatial, and the unstructured effect 90% CI included zero for all neighbourhoods.

For the statistical analysis, we used R version 3.6.1 [42] and packages RStan [51] and loo, which was used to obtain the WAIC [52]. The R script and models codes in Stan are available at https://github.com/laispfreitas/ICAR_chikungunya [53]. Maps and graphs were created using QGIS version 3.12 [54] and ggplot2 version 3.2.0 [55].

Ethics Statement

This study was approved by the Research Ethics Committee of Escola Nacional de Saúde Pública Sergio Arouca (ENSP) – Fundação Oswaldo Cruz, approval number 2.879.430. Informed consent was not required as this is a study using secondary data and the data were analysed anonymously.

Results

Between January and December 2016, 13,627 cases of chikungunya were notified in the city of Rio de Janeiro, corresponding to an incidence of 21.6 cases per 10,000 inhabitants. The number of cases peaked at week 17/2016, with 1118 chikungunya cases (Fig 3A). The cumulative number of cases by neighbourhood ranged from 0 (Grumari, area 4.0) to 721 (Realengo, area 5.1). The highest incidence was found in Catumbi (area 1.0), of 211.0 cases per 10,000 inhabitants (Fig 3B).

Fig 3. Notified chikungunya cases by week (A) and chikungunya cases cumulative incidence per 10,000 inhabitants by neighbourhood (B), January to December 2016, Rio de Janeiro city, Brazil.

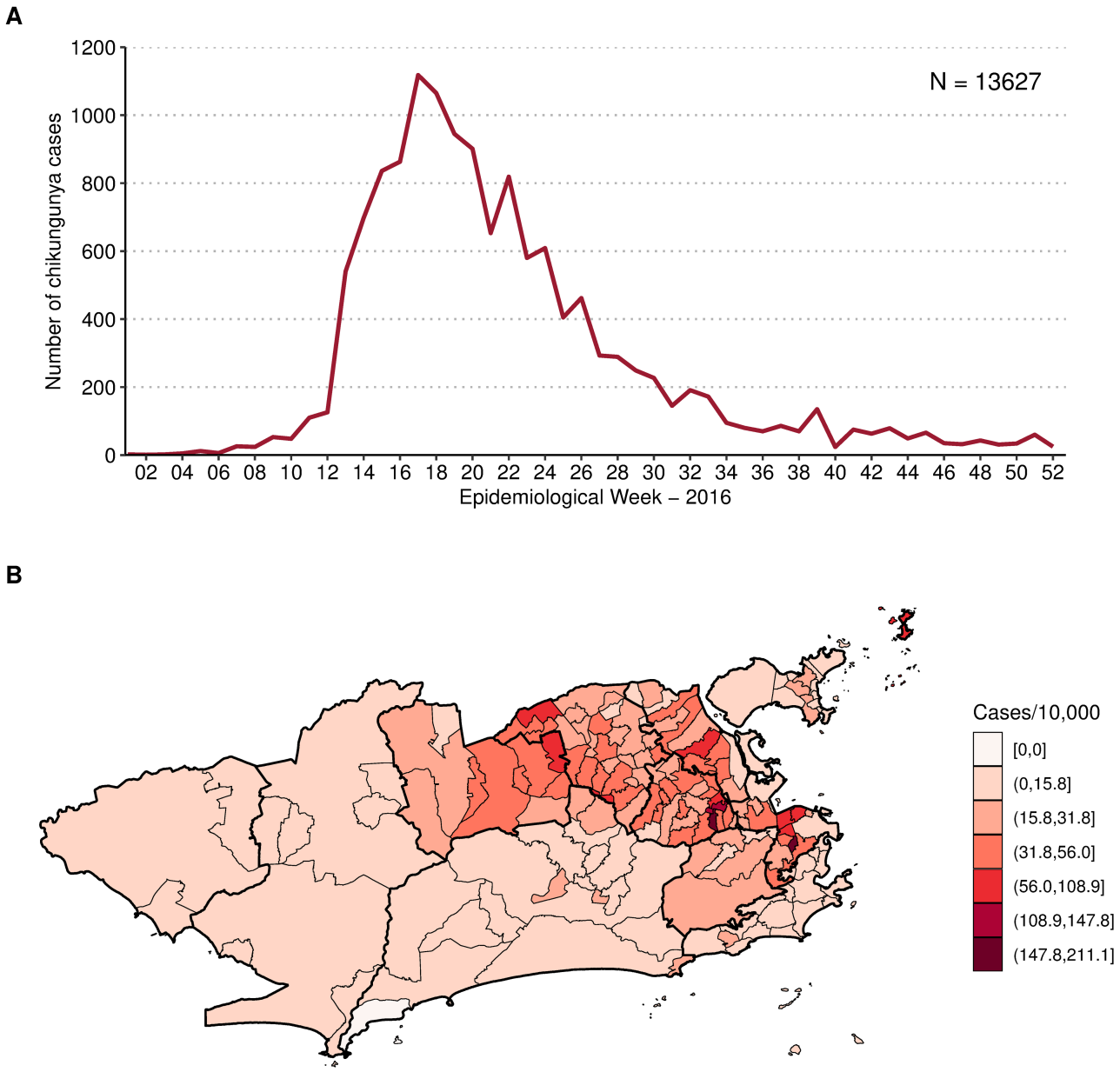

The mean sociodevelopment index was 0.6080, ranging from 0.282 in Grumari (area 4.0) to 0.819 in Lagoa (area 2.1). Higher sociodevelopment indexes were observed in the areas 2.1 and 4.0 (Fig 4A). Fifteen neighbourhoods did not have any green areas, mostly located in areas 1.0, 3.1, 3.2

and 3.3 (Fig 4B). Alto da Boa Vista (area 2.2) presented the highest percentage of green areas, of 90.4%. The average minimum temperature was 19.9 °C, ranging from 10.7 °C in Campo dos Afonsos (area 5.1) to 26.1 °C in Cidade Nova (area 1.0). Neighbourhoods in the east coastal region of Rio had higher temperatures on average (Fig 4C). The temperature decreased in the city around week 17, starting to increase again around week 35 (Fig 4D).

Fig 4. Sociodevelopment index in 2010 (A), percentage of green areas in 2015 (B), minimum temperature (ºC) average in 2016 by neighbourhood (C) and boxplot of the minimum temperature (ºC) by neighbourhood and week (D), Rio de Janeiro city, Brazil.

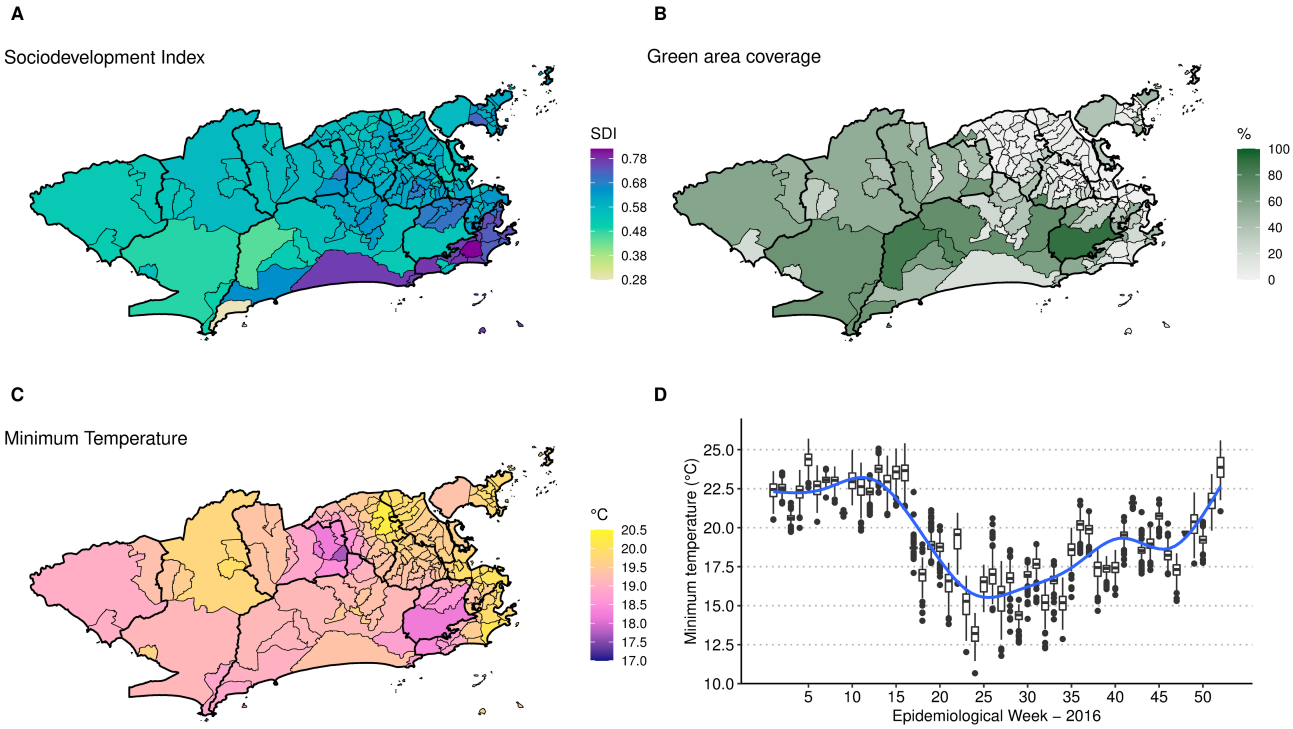

Due to the small numbers of chikungunya cases at the beginning of 2016, we decided to model the cases starting at week 9, when the number of cases in the city exceeded 50 for the first time.

The posterior summary (mean and 90% CI) of the time-varying coefficients for sociodevelopment index and proportion of green areas is presented in Fig 5. The sociodevelopment index presented a strong protective effect at the beginning of the epidemic. The sociodevelopment

index effect was inversely associated with the epidemic curve: as the number of cases increased, the protective effect decreased, remaining almost constant during the peak of the epidemic, and increasing again once the number of cases started decreasing. The effect of the sociodevelopment index was null during the peak of the epidemic (around week 17). The proportion of green areas effect included 0 in the 90% CI in most of the weeks. However, when the spatial component was not included in the model, it presented a protective effect (Fig C in S2 Fig).

Fig 5. Time-varying coefficients (in the log scale, mean and 90% credible interval) for sociodevelopment index (SDI) (A) and proportion of green areas (B) for a spatial model for chikungunya cases from weeks 9 to 52 2016 and controlling for minimum temperature, Rio de Janeiro city, Brazil.

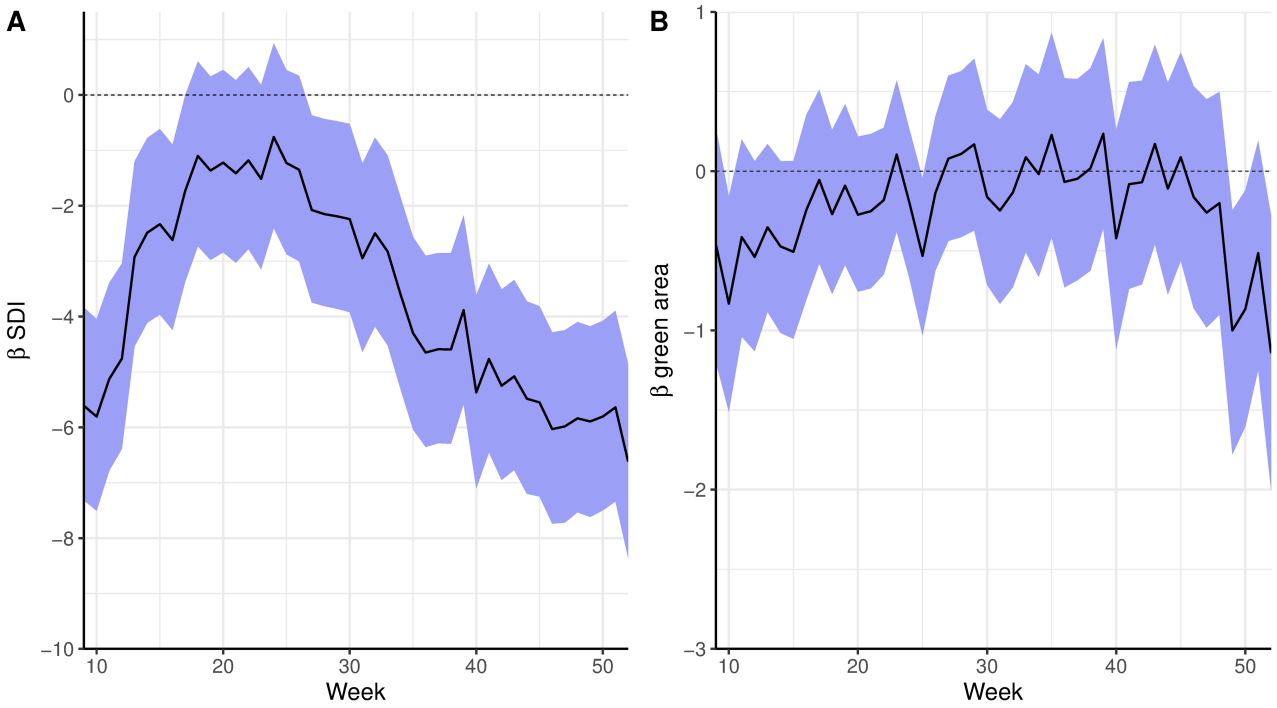

The latent spatial structure has a clear trend of positive spatial effects in areas where the epidemic was concentrated (areas 1.0, 2.2, the mainland part of 3.1, 3.2, 3.3 and 5.1) and negative spatial effects in less affected areas (Fig 6). The inclusion of the covariates in the final model

283 decreased the spatial effects in 102 of the 160 neighbourhoods compared to the model with only the
284 spatial effect (S3 Fig).

285 **Fig 6. Chikungunya cases mean spatial effects (in the log scale) controlling for**
286 **sociodevelopment index, proportion of green areas, and minimum temperature, weeks 9 to 52**
287 **2016, Rio de Janeiro city, Brazil.**

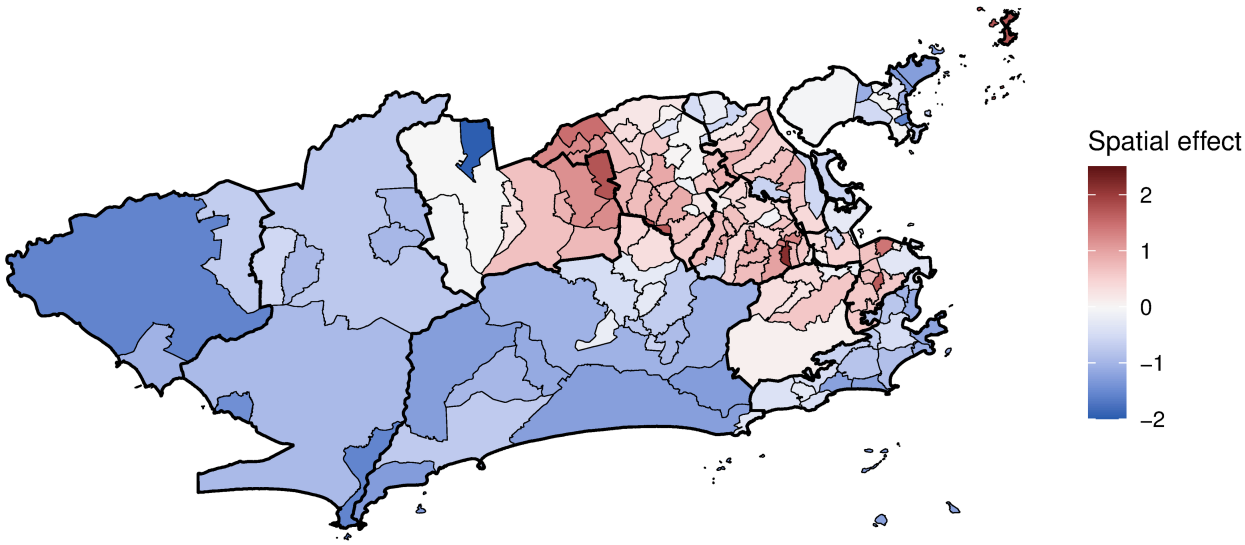

289 The posterior distributions (mean and 90% CI) of the instantaneous and memory effects of
290 the minimum temperature are displayed in Fig 7. For most neighbourhoods (113/160, or 70.6%) the
291 instantaneous effect of the temperature increased the risk of chikungunya cases (Fig 7A). The
292 instantaneous temperature effect, however, was in general small, reaching its maximum in Catumbi
293 (area 1.0), where the temperature relative risk was 2.28 (90%CI 2.07-2.53). The memory effect (Fig
294 7B) represents the propagation in time of the instantaneous effect. Therefore, in neighbourhoods
295 where the instantaneous temperature effect was null, the memory effect is irrelevant.
296

Fig 7. Minimum temperature instantaneous effect (in the same week) (A) and memory effect (B) on chikungunya cases (in the log scale) by neighbourhood, mean and 90% credible interval, controlling for sociodevelopment index and proportion of green areas, and the latent spatial effect, weeks 9 to 52 2016, Rio de Janeiro city, Brazil.

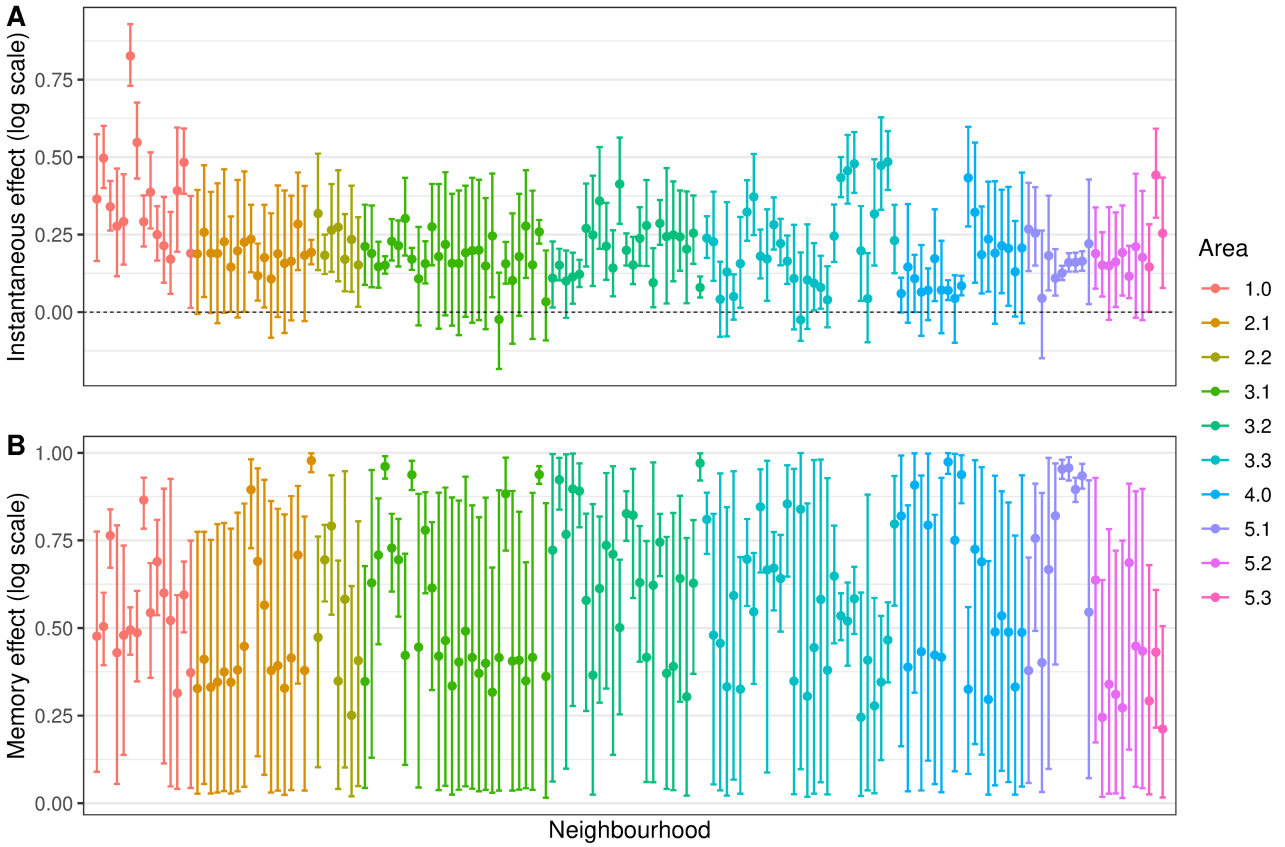

The combined effect of the minimum temperature, represented by the impulse response function, presented three patterns. These patterns are exemplified with nine selected neighbourhoods in Fig 8: null effect (Fig 8 first row), rapid decay of the effect (second row), and slow decay of the effect (third row). The impulse response functions for all neighbourhoods are available in the S4 Fig.

Fig 8. Impulse response function of the minimum temperature effect on chikungunya cases over time, posterior mean and 90% credible interval, controlling for sociodevelopment index and proportion of green areas, and the latent spatial effect, in selected neighbourhoods, Rio de Janeiro city, Brazil.

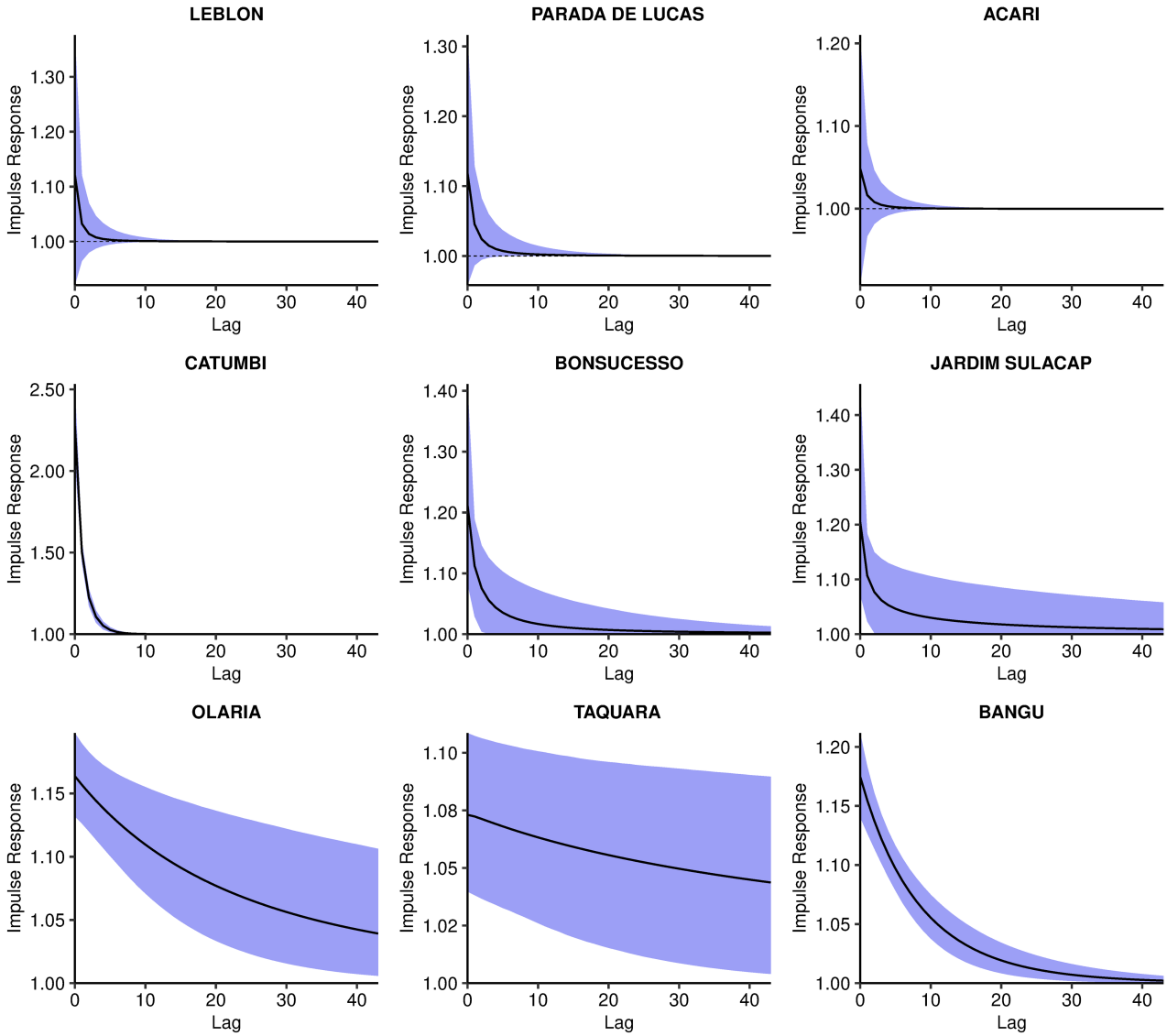

The impulse response function is represented in time and space in Fig 9 and S1 Video. The first map depicts the mean temperature instantaneous relative risk, the impulse. The following maps show the propagation of the impulse on subsequent weeks. When the temperature relative risk is null (90% CI includes the 1), the neighbourhood is depicted blank. The strong memory effect in

some neighbourhoods (Fig 7B) is observed by the persistence of the temperature effect for several weeks after the impulse. However, such effect declines to values very close to 1. These neighbourhoods were concentrated in the areas 1.0, 2.2, mainland 3.1, 3.2, 3.3 and 5.1.

Fig 9. Minimum temperature instantaneous effect on chikungunya cases and its propagation in time by neighbourhood in selected weeks, controlling for sociodevelopment index and green areas proportion, and the latent spatial effect, Rio de Janeiro city, Brazil.

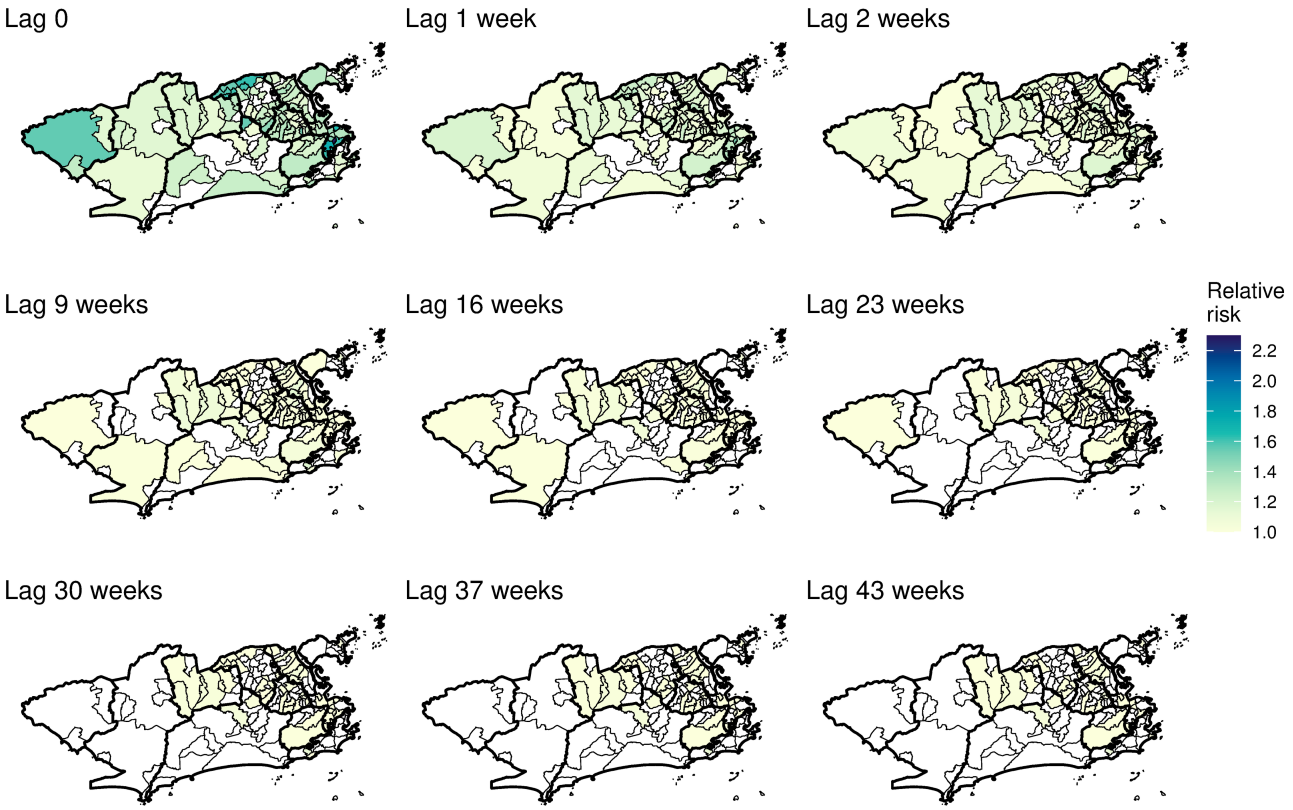

The mean estimated chikungunya relative risk increased rapidly in the first weeks, peaking at week 17 and then decaying progressively (S2 Video and Fig 10). The decrease in the chikungunya relative risk coincided with the decrease in the minimum temperature in the city (Fig 4D). High relative risks for chikungunya were mostly observed in the areas 1.0, 2.2, 3.1, 3.2, 3.3 and 5.1. The neighbourhoods of the remaining areas presented chikungunya relative risks below 1 for almost the

329 entire study period. The classification of the neighbourhoods in terms of chikungunya relative risk
330 considering the 90% CI is available in the S5 Fig.

331 **Fig 10. Posterior mean chikungunya relative risk by neighbourhood in selected weeks,**
332 **controlling for sociodevelopment index, proportion of green areas, and minimum**
333 **temperature, and the latent spatial effect, Rio de Janeiro city, Brazil.**

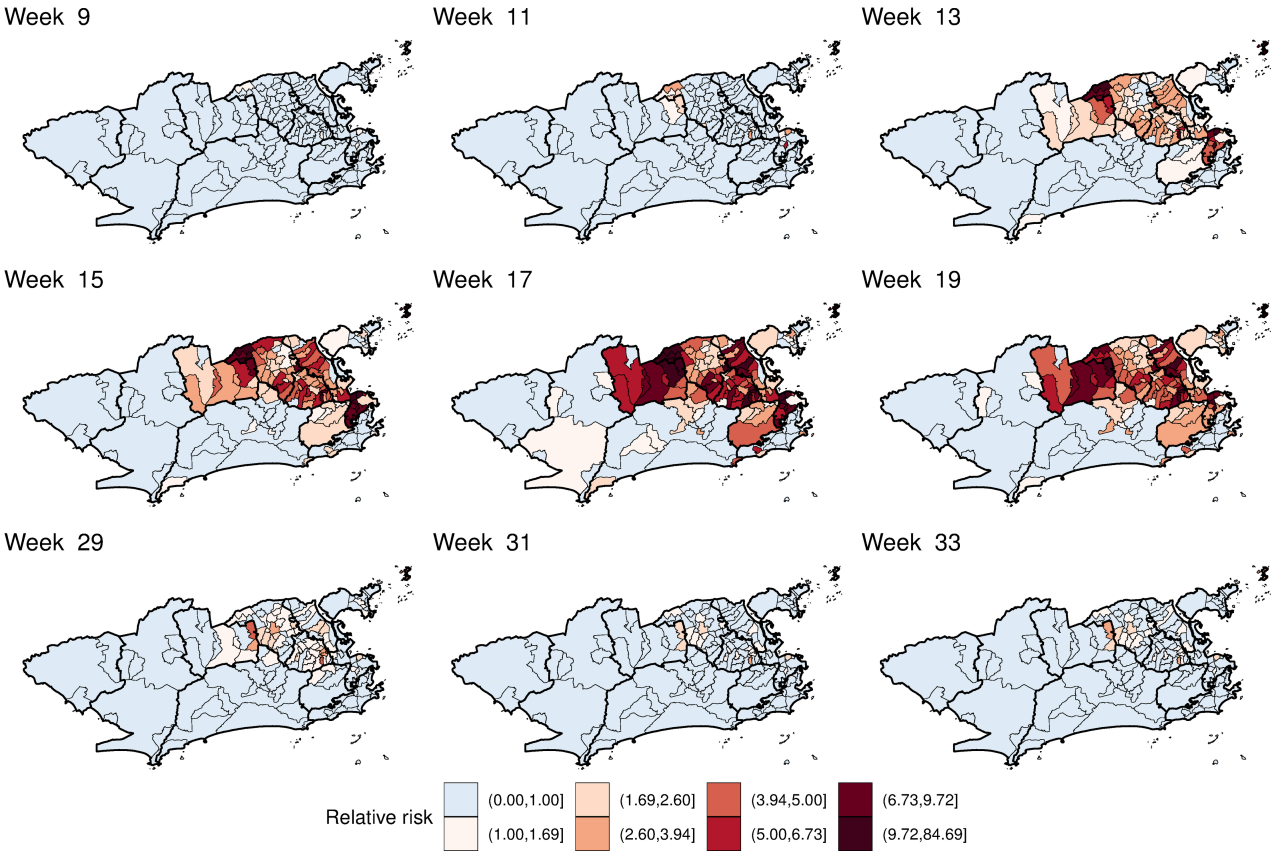

335 ## Discussion

336 In this study, we estimated the associaton of socioeconomic status, environment, and
337 temperature with the spatio-temporal distribution of the first chikungunya epidemic in Rio de
338 Janeiro city. The sociodevelopment index and the proportion of green areas were included in the
339 model with time-varying coefficients, allowing us to explore how the effects of these factors
340 changed throughout the epidemic. The temperature was included in the model in a non-linear
341 fashion using a transfer function, considering that the temperature has an immediate effect and that

342 a proportion of this effect propagates to future times. To our knowledge, this is the first time a
343 transfer function is applied for temperature when modelling *Aedes*-borne diseases.

344 The sociodevelopment index was inversely associated with the risk of chikungunya in all
345 models (Fig 5A, Figs A and B in S2 Fig). In fact, the sociodevelopment index presented the
346 strongest effect in the models, which strengthens the hypothesis of chikungunya being a disease of
347 social determination. This index is composed of sanitary conditions indicators, among others, and
348 poor sanitary conditions are known to favour the reproduction of the *Ae. aegypti* mosquitoes. The
349 association of low socioeconomic locations with increased risk of chikungunya was also found in a
350 study in French Guiana [56] and in a study in Barraquilla, a Colombian city [21]. Our results
351 indicate that poor neighbourhoods were affected first and hardest by the chikungunya epidemic,
352 highlighting the importance of vector control activities in socioeconomically vulnerable locations.

353 When the spatial dependency was not included in the model, the proportion of green areas
354 was negatively associated with the number of chikungunya cases (Fig C in S2 Fig). Such
355 association was observed for dengue in São Paulo, where low vegetation cover areas presented
356 higher dengue incidence rates [22]. However, with the inclusion of the spatial component, the effect
357 of the proportion of green areas moved towards the null. This is possible due to spatial confounding,
358 which happens when covariates that are spatially smooth are collinear with spatial random effects
359 [57]. In Rio de Janeiro, the majority of the green areas are in the mountain massifs (Fig 2), which
360 trespasses different neighbouring borders.

361 The temperature was associated with an increase in the risk of chikungunya in most
362 neighbourhoods. In our models, we assumed that the temperature presents an effect that is a
363 combination of an instantaneous effect and of a proportion of this that propagates in time (the
364 memory effect). Although the instantaneous association is relatively low across the different
365 neighbourhoods, it can persist for a long period of time for some of the districts. This was only
366 possible because we allowed the parameters present in the transfer function to change across

neighbourhoods. Different areas experiencing heterogeneous temperature effects for *Aedes*-borne diseases were also observed in previous studies [58,59]. The inclusion of space-varying coefficients for the temperature improved the fitting of our models.

The instantaneous association represents the effect of the temperature on the activity of the mosquito, human behaviour and the mosquito-virus interaction. The biting rate of the *Ae. aegypti* increases with the temperature until around 35 °C [10], and people become more exposed to mosquitoes in warm temperatures. The temperature also accelerates the virus extrinsic incubation period in the mosquito, and transmission was estimated to peak around 28.5 °C [10]. On the other hand, the temperature affects the population of mosquitoes by increasing fecundity, egg-to-adult-survival, development rate and lifespan [10]. This effect is not only on the same week but also accumulates in time, which is captured by the memory effect.

Interestingly, the CHIKV epidemic in Rio de Janeiro in 2016 did not reach the whole city, with high-risk areas mostly concentrated in the North and Downtown regions. The decrease in the number of cases coincided with the drop in the minimum temperature, around week 17 (Fig 3A and 4D). These two observations combined suggest that the epidemic was interrupted not because of susceptible human population depletion in the city, but because the drop in temperature caused a reduction in the transmission in such a way that the epidemic was not sustained. It is important to note that although the number of cases diminished substantially, there were still chikungunya cases being reported until the end of the year. Rio de Janeiro is a tropical city, and the minimum temperature rarely is below the minimum temperature needed for transmission to occur, of 13.5 °C [10]. A previous study conducted in the city showed that the *Ae. aegypti* population varies seasonally, but the mosquito is endemic all over the year [60]. This could explain the long persistence of the temperature effect in time in some neighbourhoods (Fig 9 and S1 Video).

The application of spatial models considering intra-urban scenarios is still growing for *Aedes*-borne diseases. Our study identified high-risk neighbourhoods for the first chikungunya

392 epidemic in Rio de Janeiro city, which concentrated mostly in the North and Downtown regions
393 (Fig 10 and S2 Video). Such regions were already identified as high-risk locations for dengue [61].
394 In our previous study, neighbourhoods from these regions were more likely to constitute
395 simultaneous clusters for dengue, Zika and chikungunya [62]. These regions have a combination of
396 factors that favours the *Ae. aegypti*'s ecology and transmission of diseases: low vegetation, low
397 socioeconomic status and increased temperature (Fig 4). Vector control activities should be
398 prioritised and intensified in the identified high-risk areas, as they also appear to be the first ones
399 affected by the epidemic. Additionally, the long persistence of the temperature effect (Fig 9 and S1
400 Video) and a small number of cases even after the decline of the epidemic, indicate that the
401 mosquito continues to circulate and to transmit the disease throughout the year. Therefore,
402 interventions must be designed to be continuous and to work in the long term in these locations.

403 Our study has some limitations. As for any study using secondary data on *Aedes*-borne
404 diseases, there is an uncertainty on the diagnosis of the reported cases as well as under-reporting. It
405 is important to consider that, in the same year, the city was also experiencing dengue and Zika
406 epidemics [62]. Because of the association between Zika and severe congenital manifestations, the
407 disease awareness around Zika may have improved the reporting rates [63]. However, the
408 simultaneous occurrence of three arbovirus epidemics may have impaired the differential diagnosis,
409 as they cause similar symptoms. Another limitation is the spatial unit. We analysed the data
410 aggregated at the neighbourhood level. Although the data are more reliable at this spatial unit,
411 smaller areas inside the same neighbourhood can present different socioeconomic and
412 environmental characteristics. Finer scales such as census tracts should be considered in future
413 studies. Finally, an important limitation is the assumption that the chikungunya risk is related to the
414 neighbourhood of residence, while some people may get infected in other locations.

415 The model here presented has the potential to be applied to other cities and other urban
416 *Aedes*-borne diseases. Mosquito population information is expensive to collect and often unreliable.

Therefore not depending on such data is a strength of our model. Another strength is the application of a transfer function to estimate the non-linear effect of the temperature and its duration. By using temperature, socioeconomic status and proportion of green areas data as proxies of the key elements of CHIKV transmission, our model contributed to understanding better the spatio-temporal dynamics of the first chikungunya epidemic in a tropical metropolitan city. Importantly, our results indicate that even considering the environment and the temperature, the socioeconomic status plays a major role in affecting the incidence and distribution of a first *Aedes*-borne disease epidemic in a large city. This strengthens the importance of improving sanitary conditions and taking measures to diminish social inequality as necessary actions to control and prevent *Aedes*-borne diseases.

Acknowledgements

The authors would like to thank the Municipal Secretariat of Health for providing the data on reported cases, and the meteorological and environmental institutes (INMET, DECEA, INEA, SMAC and *Alerta Rio*), for making their meteorological data publicly available. We are grateful for support from the Coordination for the Improvement of Higher Education Personnel (CAPES).

References

1. de Souza T, Ribeiro E, Corrêa V, Damasco P, Santos C, de Bruycker-Nogueira F, et al. Following in the Footsteps of the Chikungunya Virus in Brazil: The First Autochthonous Cases in Amapá in 2014 and Its Emergence in Rio de Janeiro during 2016. Viruses. 2018;10: 623. doi:10.3390/v10110623

2. WHO. Chikungunya. In: World Health Organization [Internet]. 12 Apr 2017 [cited 16 Jul 2018]. Available: http://www.who.int/news-room/fact-sheets/detail/chikungunya

3. Honório NA, Nogueira RMR, Codeço CT, Carvalho MS, Cruz OG, Magalhães M de AFM, et al. Spatial Evaluation and Modeling of Dengue Seroprevalence and Vector Density in Rio de Janeiro, Brazil. Gubler D, editor. PLoS Neglected Tropical Diseases. 2009;3: e545. doi:10.1371/journal.pntd.0000545

4. Nogueira RMR, Miagostovich MP, Schatzmayr HG, Santos FB dos, Araújo ESM de, Filippis AMB de, et al. Dengue in the State of Rio de Janeiro, Brazil, 1986-1998. Memórias do Instituto Oswaldo Cruz. 1999;94: 297–304. doi:10.1590/S0074-02761999000300004

5. Santos JPC dos, Honório NA, Nobre AA. Definition of persistent areas with increased dengue risk by detecting clusters in populations with differing mobility and immunity in Rio de Janeiro, Brazil. Cadernos de Saúde Pública. 2019;35. doi:10.1590/0102-311x00248118

6. Kuno G. Review of the Factors Modulating Dengue Transmission. Epidemiologic Reviews. 1995;17: 321–335. doi:10.1093/oxfordjournals.epirev.a036196

7. Randolph SE, Rogers DJ. The arrival, establishment and spread of exotic diseases: patterns and predictions. Nature Reviews Microbiology. 2010;8: 361–371. doi:10.1038/nrmicro2336

8. Teixeira MG, Costa M da CN, Barreto F, Barreto ML. Dengue: twenty-five years since reemergence in Brazil. Cadernos de Saúde Pública. 2009;25: S7–S18. doi:10.1590/S0102-311X2009001300002

9. Zouache K, Fontaine A, Vega-Rua A, Mousson L, Thiberge J-M, Lourenco-De-Oliveira R, et al. Three-way interactions between mosquito population, viral strain and temperature underlying chikungunya virus transmission potential. Proceedings of the Royal Society B: Biological Sciences. 2014;281: 20141078. doi:10.1098/rspb.2014.1078

10. Mordecai EA, Cohen JM, Evans MV, Gudapati P, Johnson LR, Lippi CA, et al. Detecting the impact of temperature on transmission of Zika, dengue, and chikungunya using mechanistic models. Althouse B, editor. PLOS Neglected Tropical Diseases. 2017;11: e0005568. doi:10.1371/journal.pntd.0005568

11. Rosa-Freitas MG, Tsouris P, Reis IC, Magalhães M de AFM, Nascimento TFS, Honório NA. Dengue land cover heterogeneity in Rio de Janeiro. Oecologia Australis. 2010;14: 641–667. doi:10.4257/oeco.2010.1403.04

12. Carvalho MS, Honorio NA, Garcia LMT, Carvalho LC de S. Aedes ægypti control in urban areas: A systemic approach to a complex dynamic. Reiner RC, editor. PLOS Neglected Tropical Diseases. 2017;11: e0005632. doi:10.1371/journal.pntd.0005632

13. Honório NA, Castro MG, Barros FSM de, Magalhães M de AFM, Sabroza PC. The spatial distribution of Aedes aegypti and Aedes albopictus in a transition zone, Rio de Janeiro, Brazil. Cadernos de Saúde Pública. 2009;25: 1203–1214. doi:10.1590/S0102-311X2009000600003

14. Flauzino RF, Souza-Santos R, Oliveira RM. Dengue, geoprocessamento e indicadores socioeconômicos e ambientais: um estudo de revisão. Revista Panamericana de Salud Pública. 2009;25: 456–461. doi:10.1590/S1020-49892009000500012

15. Carvalho MS, Freitas LP, Cruz OG, Brasil P, Bastos LS. Association of past dengue fever epidemics with the risk of Zika microcephaly at the population level in Brazil. Scientific Reports. 2020;10. doi:10.1038/s41598-020-58407-7

16. Lowe R, Gasparrini A, Van Meerbeeck CJ, Lippi CA, Mahon R, Trotman AR, et al. Nonlinear and delayed impacts of climate on dengue risk in Barbados: A modelling study. Thomson M, editor. PLOS Medicine. 2018;15: e1002613. doi:10.1371/journal.pmed.1002613

17. Lowe R, Bailey TC, Stephenson DB, Graham RJ, Coelho CAS, Sá Carvalho M, et al. Spatio-temporal modelling of climate-sensitive disease risk: Towards an early warning system for dengue in Brazil. Computers & Geosciences. 2011;37: 371–381. doi:10.1016/j.cageo.2010.01.008

18. Puggioni G, Couret J, Serman E, Akanda AS, Ginsberg HS. Spatiotemporal modeling of dengue fever risk in Puerto Rico. Spatial and Spatio-temporal Epidemiology. 2020;35: 100375. doi:10.1016/j.sste.2020.100375

19. Martínez-Bello D, López-Quílez A, Torres Prieto A. Spatio-Temporal Modeling of Zika and Dengue Infections within Colombia. International Journal of Environmental Research and Public Health. 2018;15: 1376. doi:10.3390/ijerph15071376

20. Martínez-Bello DA, López-Quílez A, Torres Prieto A. Relative risk estimation of dengue disease at small spatial scale. International Journal of Health Geographics. 2017;16. doi:10.1186/s12942-017-0104-x

21. McHale TC, Romero-Vivas CM, Fronterre C, Arango-Padilla P, Waterlow NR, Nix CD, et al. Spatiotemporal Heterogeneity in the Distribution of Chikungunya and Zika Virus Case Incidences during their 2014 to 2016 Epidemics in Barranquilla, Colombia. International Journal of Environmental Research and Public Health. 2019;16: 1759. doi:10.3390/ijerph16101759

22. Teixeira TR de A, Cruz OG. Spatial modeling of dengue and socio-environmental indicators in the city of Rio de Janeiro, Brazil. Cadernos de Saúde Pública. 2011;27: 591–602. doi:10.1590/S0102-311X2011000300019

23. Besag J. Spatial Interaction and the Statistical Analysis of Lattice Systems. Journal of the Royal Statistical Society Series B (Methodological). 1974;36: 192–236.

24. Morris M, Wheeler-Martin K, Simpson D, Mooney SJ, Gelman A, DiMaggio C. Bayesian hierarchical spatial models: Implementing the Besag York Mollié model in stan. Spatial and Spatio-temporal Epidemiology. 2019;31: 100301. doi:10.1016/j.sste.2019.100301

25. Alves MB, Gamerman D, Ferreira MA. Transfer functions in dynamic generalized linear models. Statistical Modelling: An International Journal. 2010;10: 03–40. doi:10.1177/1471082X0801000102

26. Prefeitura do Rio de Janeiro. Rio em Síntese. In: Data Rio [Internet]. [cited 11 Jun 2018]. Available: http://www.data.rio/pages/rio-em-sntese-2

27. Cavallieri F, Vial A. Favelas na cidade do Rio de Janeiro: o quadro populacional com base no Censo 2010. Rio de Janeiro, RJ: Instituto Pereira Passos; 2012 p. 20. Report No.: 20120501. Available: http://portalgeo.rio.rj.gov.br/estudoscariocas/download%5C3190_FavelasnacidadedoRiodeJaneiro_Censo_2010.PDF

28. Prefeitura do Rio de Janeiro, Secretaria Municipal de Saúde. Chikungunya. Available: http://www.rio.rj.gov.br/web/sms/exibeConteudo?id=4769664

29. Ministério da Saúde. Chikungunya: manejo clínico. Brasília, DF; 2017. Available: http://bvsms.saude.gov.br/bvs/publicacoes/chikungunya_manejo_ clinico_1ed.pdf

30. Prefeitura do Rio de Janeiro. Índice de Desenvolvimento Social (IDS) por Áreas de Planejamento (AP), Regiões de Planejamento (RP), Regiões Administrativas (RA), Bairros e Favelas do Município do Rio de Janeiro - 2010. In: Data Rio [Internet]. 29 May 2019 [cited 10 Sep 2019]. Available: http://www.data.rio/datasets/fa85ddc76a524380ad7fc60e3006ee97

31. Prefeitura do Rio de Janeiro. População residente, por idade e por grupos de idade, segundo as Áreas de Planejamento (AP), Regiões Administrativas (RA) e Bairros em 2000/2010. In: Data Rio [Internet]. 30 May 2019 [cited 10 Sep 2019]. Available: http://www.data.rio/datasets/e68e54eaa6bb484dbb40828acf2b3e7e

32. Prefeitura do Rio de Janeiro. Uso do Solo 2015. In: Data Rio [Internet]. 18 Jul 2019 [cited 10 Sep 2019]. Available: http://www.data.rio/datasets/e74a94ac95d440d19b3e18c23bc485de_6

33. INMET. Estações Automáticas. In: INMET - Instituto Nacional de Meteorologia [Internet]. [cited 24 May 2020]. Available: http://www.inmet.gov.br/portal/index.php?r=estacoes/estacoesAutomaticas

34. DECEA. REDEMET - Painel de consulta. In: Rede de Meteorologia do Comando da Aeronáutica [Internet]. [cited 25 May 2020]. Available: https://www.redemet.aer.mil.br/?i=produtos&p=consulta-de-mensagens-opmet

35. INEA. Dados do Monitoramento da Qualidade do Ar e Meteorologia. In: Instituto Estadual do Ambiente Rio de Janeiro [Internet]. [cited 24 May 2020]. Available: http://200.20.53.25/qualiar/home/index

36. SMAC. Dados horários do monitoramento da qualidade do ar - MonitorAr. In: Data Rio [Internet]. [cited 25 May 2020]. Available: http://www.data.rio/datasets/dados-hor%C3%A1rios-do-monitoramento-da-qualidade-do-ar-monitorar?orderBy=Data

37. Prefeitura do Rio de Janeiro. Dados Meteorológicos. In: Sistema Alerta Rio [Internet]. [cited 24 May 2020]. Available: http://alertario.rio.rj.gov.br/download/dados-meteorologicos/

38. World Meteorological Organization, editor. Guide to the global observing system. 3rd ed. Geneva: World Meteorological Organization; 2007.

39. Gomes AF, Nobre AA, Cruz OG. Temporal analysis of the relationship between dengue and meteorological variables in the city of Rio de Janeiro, Brazil, 2001-2009. Cadernos de Saúde Pública. 2012;28: 2189–2197. doi:10.1590/S0102-311X2012001100018

40. Lowe R, Stewart-Ibarra AM, Petrova D, García-Díez M, Borbor-Cordova MJ, Mejía R, et al. Climate services for health: predicting the evolution of the 2016 dengue season in Machala, Ecuador. The Lancet Planetary Health. 2017;1: e142–e151. doi:10.1016/S2542-5196(17)30064-5

41. Diggle P, Ribeiro PJ. Model-based Geostatistics. New York: Springer-Verlag; 2007. doi:10.1007/978-0-387-48536-2

42. The R Foundation for Statistical Computing. R. The R Foundation; 2020. Available: https://www.r-project.org/

43. Pebesma E, Bivand R, Racine E, Sumner M, Cook I, Keitt T, et al. sf: Simple Features for R. 2019. Available: https://CRAN.R-project.org/package=sf

44. Ribeiro PJ, Diggle PJ. geoR: A Package for Geostatistical Analysis. R-NEWS. 2001;1: 15–18.

45. Wickham H, RStudio. tidyverse: Easily Install and Load the “Tidyverse.” 2017. Available: https://CRAN.R-project.org/package=tidyverse

46. Stan Development Team. Stan Reference Manual. Version 2.23. Available: https://mc-stan.org/docs/2_23/reference-manual/notation-for-samples-chains-and-draws.html

47. Carpenter B, Gelman A, Hoffman MD, Lee D, Goodrich B, Betancourt M, et al. *Stan*: A Probabilistic Programming Language. Journal of Statistical Software. 2017;76. doi:10.18637/jss.v076.i01

48. Watanabe S. Asymptotic Equivalence of Bayes Cross Validation and Widely Applicable Information Criterion in Singular Learning Theory. 2010; 24.

49. Gelman A, Rubin DB. Inference from Iterative Simulation Using Multiple Sequences. Statistical Science. 1992;7: 457–472. doi:10.1214/ss/1177011136

50. Riebler A, Sørbye SH, Simpson D, Rue H. An intuitive Bayesian spatial model for disease mapping that accounts for scaling: Statistical Methods in Medical Research. 2016 [cited 29 Apr 2020]. doi:10.1177/0962280216660421

51. Guo J, Gabry J, Goodrich B, Lee D, Sakrejda K, Martin M, et al. rstan: R Interface to Stan. 2019. Available: https://CRAN.R-project.org/package=rstan

52. Vehtari A, Gelman A, Gabry J. Practical Bayesian model evaluation using leave-one-out cross-validation and WAIC. Statistics and Computing. 2017;27: 1413–1432. doi:10.1007/s11222-016-9696-4

53. Freitas LP, Schmidt AM. laispfreitas/ICAR_chikungunya: The role of socioeconomic status, environment, and temperature in the spatio-temporal distribution of the first Chikungunya epidemic in the city of Rio de Janeiro, Brazil. Zenodo; 2020. doi:10.5281/ZENODO.3936204

54. QGIS Development Team. QGIS Geographic Information System. Open Source Geospatial Foundation Project; 2020. Available: https://qgis.org/en/site/

55. Wickham H. ggplot2: Elegant Graphics for Data Analysis. Springer-Verlag. 2016. Available: https://ggplot2.tidyverse.org/

56. Bonifay T, Douine M, Bonnefoy C, Hurpeau B, Nacher M, Djossou F, et al. Poverty and Arbovirus Outbreaks: When Chikungunya Virus Hits More Precarious Populations Than Dengue Virus in French Guiana. Open Forum Infectious Diseases. 2017;4. doi:10.1093/ofid/ofx247

57. Clayton DG, Bernardinelli L, Montomoli C. Spatial Correlation in Ecological Analysis. International Journal of Epidemiology. 1993;22: 1193–1202. doi:10.1093/ije/22.6.1193

58. Xu Z, Bambrick H, Yakob L, Devine G, Lu J, Frentiu FD, et al. Spatiotemporal patterns and climatic drivers of severe dengue in Thailand. Science of The Total Environment. 2019;656: 889–901. doi:10.1016/j.scitotenv.2018.11.395

59. Lauer SA, Sakrejda K, Ray EL, Keegan LT, Bi Q, Suangtho P, et al. Prospective forecasts of annual dengue hemorrhagic fever incidence in Thailand, 2010–2014. Proceedings of the National Academy of Sciences. 2018;115: E2175–E2182. doi:10.1073/pnas.1714457115

60. Honório NA, Codeço CT, Alves FC, Magalhães M de AFM, Lourenço-de-Oliveira R. Temporal Distribution of *Aedes aegypti* in Different Districts of Rio De Janeiro, Brazil,

Measured by Two Types of Traps. Journal of Medical Entomology. 2009;46: 1001–1014. doi:10.1603/033.046.0505

61. Xavier DR, Magalhães M de AFM, Gracie R, Reis IC dos, Matos VP de, Barcellos C. Difusão espaço-tempo do dengue no Município do Rio de Janeiro, Brasil, no período de 2000-2013. Cadernos de Saúde Pública. 2017;33. doi:10.1590/0102-311x00186615

62. Freitas LP, Cruz OG, Lowe R, Sá Carvalho M. Space–time dynamics of a triple epidemic: dengue, chikungunya and Zika clusters in the city of Rio de Janeiro. Proceedings of the Royal Society B: Biological Sciences. 2019;286: 20191867. doi:10.1098/rspb.2019.1867

63. Lowe R, Barcellos C, Brasil P, Cruz OG, Honório NA, Kuper H, et al. The Zika Virus Epidemic in Brazil: From Discovery to Future Implications. International Journal of Environmental Research and Public Health. 2018;15: 96. doi:10.3390/ijerph15010096

S1 Fig. Meteorological weather stations (red dots) in the 500m X 500m grid and neighbourhoods, Rio de Janeiro city, Brazil.

S1 Appendix. Models structures explored to estimate $\mu_{i,t}$ and each Watanabe-Akaike information criterion (WAIC).

S2 Fig. Time-varying coefficients (in the log scale, mean and 90% credible interval) for sociodevelopment index (SDI) (A,B) and proportion of green areas (C,D) without (model 1) and with (model 2) spatial dependency, for chikungunya cases from weeks 9 to 52 2016, Rio de Janeiro city, Brazil.

S3 Fig. Correlation between the spatial effects (in the log scale) of Model 0 versus Model 4, by neighbourhood, weeks 9 to 52 2016, Rio de Janeiro city, Brazil.

S4 Fig. Impulse response of the minimum temperature, posterior mean and 90% credible interval, by neighbourhood, Rio de Janeiro city, Brazil.

S1 Video. Minimum temperature instantaneous effect on chikungunya cases and its propagation in time by neighbourhood, controlling for sociodevelopment index and proportion of green areas, and the latent spatial effect, Rio de Janeiro city, Brazil.

S2 Video. Posterior chikungunya relative risk by neighbourhood, controlling for sociodevelopment index, proportion of green areas and minimum temperature, and the latent spatial effect, weeks 9 to 52 2016, Rio de Janeiro city, Brazil.

S5 Fig. Classification of the chikungunya relative risk by neighbourhood in selected weeks based on the 90% credible interval (controlling for sociodevelopment index, proportion of green areas and minimum temperature, and the latent spatial effect), Rio de Janeiro city, Brazil. Risk: 90%CI >1. Protection: 90%CI <1. None: 90%CI includes 1.